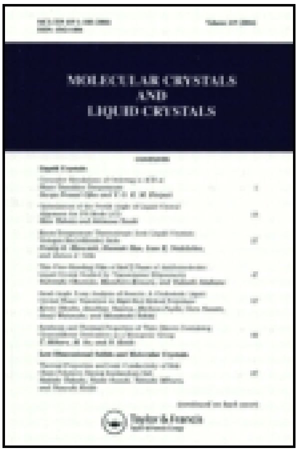

Molecular Crystals and Liquid Crystals
Publication details, including instructions for authors and subscription information:
http://www.tandfonline.com/loi/gmcl20

Structure and Stability of Molecular Layers of a Photosensitive Azo-polyacrylate by X-rays Reflectivity and GID

L. Cristofolini [a] , T. Berzina [a] , M. P. Fontana [a] & O. Konovalov [b]
[a] Dipartimento di Fisica and INFM, Università di Parma, Parma, Italy
[b] ESRF, Grenoble, France

To cite this article: L. Cristofolini, T. Berzina, M. P. Fontana & O. Konovalov (2002): Structure and Stability of Molecular Layers of a Photosensitive Azo-polyacrylate by X-rays Reflectivity and GID, Molecular Crystals and Liquid Crystals, 375:1, 689-699

To link to this article: http://dx.doi.org/10.1080/10587250210586

Mol. Cryst. Liq. Cryst., Vol. 375, pp. 689-699
Copyright © 2002 Taylor & Francis
1058-725X/02 $12.00 + .00

Structure and Stability of Molecular Layers of a Photosensitive Azo-polyacrylate by X-rays Reflectivity and GID

L. CRISTOFOLINI[a], T. BERZINA[a], M. P. FONTANA[a]
and O. KONOVALOV[b]

[a]*Dipartimento di Fisica and INFM, Università di Parma, Parma, Italy and*
[b]*ESRF, Grenoble, France*

Abstract

We report on the modifications in morphology and microscopic structure induced by photoexcitation of homo- and heterostructures of a side chain liquid crystalline polymer, namely a polyacrylate with an azobenzene moiety in the side chain. The structures were molecular mono- and multilayers deposited with the Langmuir-Schaefer technique. The structural and morphological determinations were performed with synchrotron radiation X-ray reflectometry and Grazing Incidence Diffraction (GID). We observe extensive photoinduced effects on the nanoscale: expansion of the multilayers independently of number of layers, reduction of surface roughness, and destruction of order to yield a glass-like phase. The study of superlattices composed of alternate layers of barium behenate and our polymer indicates a general reduction of photoinduced structural effects on the polymer multilayer. Finally, we discuss these effects as a function of temperature from the range of the glass transition to the clearing point.

Keywords: Polymeric liquid crystals; photoinduced effects; x-ray reflectivity.

1. INTRODUCTION

Liquid crystalline polymers with the azobenzene moiety in the side chain have been the subject of intense study in recent years [1]. Of particular interest have been the optical effects due to the photoinduced cis-trans isomerization of the azobenzene group [2]. These effects have been studied because of their potential application for optical writing and more specifically for entirely optical high density memories. The combined action of the cis-trans photoisomerization and the nematic potential lead to collective molecular reorientation phenomena, hence to very high sensitivity of the sample to the optical writing beam.
These complex molecular systems are interesting also from many other points of view. They generally form fragile glasses [3], with a very complex dynamics. A more specific point of interest is the coupling between the polymeric main chain and the mesogenic side chain [4]; this is not only at the origin of extensive optical memory effects, but also of

photomechanical relaxation over several length scales [5]. Furthermore, the different time scales which characterize the main chain and side chain dynamics add structure to the relaxation phenomena and the connected correlation functions [6].

A further point of interest for these materials is the relative ease with which form homogeneous monolayers at the air-water interface, and thus allow the monolayer or multilayer deposition onto a solid substrate using the Langmuir-Blodgett (LB) technique [7]. This paper is devoted to the study of photoinduced effects in the confined quasi-two dimensional geometry of monocomponent and heterostructure LB multilayers of side chain liquid crystalline polymers. Particular emphasis was placed on using the *cis-trans* molecular pump to study relaxation on the molecular scale. In a previous paper [8] we have reported some preliminary results obtained on LB multilayers using digital null ellipsometry. In particular, the study of photoinduced relaxation in the multilayers as a function of thickness indicated a substantial deviation from bulk behavior as the number of layers decreased to below four. This was interpreted in terms of a compacting of the structure of the first 2-4

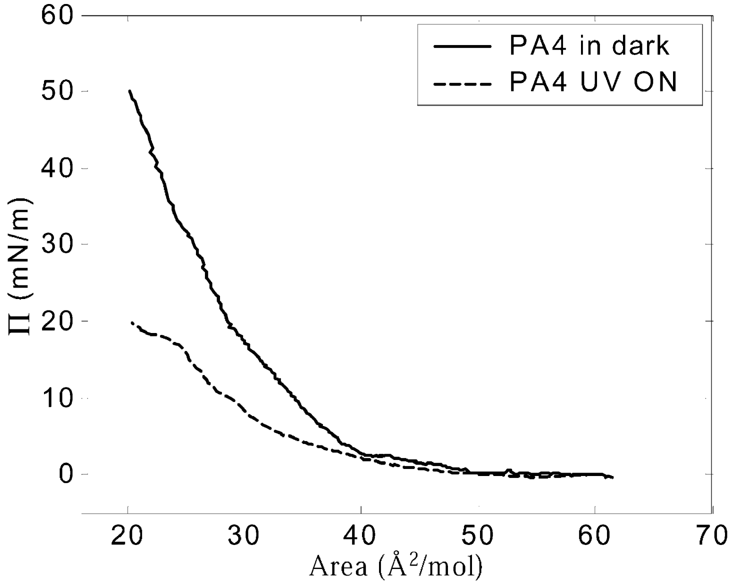

Figure 1: Compression isotherms (T=19°C) of PA4 in dark (continuous line) and under UV illumination (dotted line).

layers as T was lowered below the glass transition temperature T_g. Such effect was absent for thicker films. Furthermore, optical pumping destroyed the "crystalline" structure, restoring the glassy phase even for films with the smallest thickness (2 layers).
In this paper we extend the scope of our measurements, using synchrotron X-ray reflectometry (XRR) to determine the microscopic out-of-plane molecular arrangement in multilayers deposited onto a solid substrate and the structural and morphological changes induced by optical pumping of the photoisomerization transition of the azobenzene. The samples were homogeneous multilayers, i.e. made up of only the polymeric molecules, or they were alternate heterostructure multilayers, in which the polimeric multilayer of variable thickness was sandwiched between decoupling bilayers of barium-behenate LB films. Using these structures we could study more quantitatively the photoeffects in different geometries and confinement conditions of the liquid crystalline polymer. In particular we were able to define quantitatively the structure of the "crystallized" first 2-4 layers (the so called "dead layer") and its changes upon optical pumping.

2. EXPERIMENTAL

The liquid crystalline polymer we used was Poly[[4-pentyloxy-3'-methyl-4'(6-acryloxyexyloxy)]azobenzene] (PA4) Its synthesis and main characteristics are described elsewhere [9]. Here we recall that its has a calorimetric glass transition temperature T_g of 21° C [10], a melting temperature of 78° C, a nematic phase ending at the clearing point temperature of 96° C. Upon cooling, the nematic fluid of the azobenzene side chains undercools all the way down to T_g.

In this type of experiment, particular care must be given to the details of preparation and deposition of the LB multilayers. In particular, the samples must be as homogeneous and defect-free as possible. We found that the best results were obtained using the Langmuir-Schaefer (LS) horizontal lift deposition technique [7]. The deposited films were routinely checked with an optical polarizing microscope (Zeiss Axiotech) used also in Differential Interference Contrast (DIC) mode. Film thickness was independently measured by high precision null-ellipsometry (Multiskop). Nanoscopic surface morphology and roughness was monitored with AFM microscopy in non-contact mode (Park Autoprobe Research). Given the essential metastable character of films deposited using LB techniques, the phenomenon of de-wetting [11] must always be checked, since in particular in both ellipsometry and XRR measurements de-wetting may mimic large surface roughness. Thus the AFM characterization is useful in our experiment to check for possible de-wetting events as we vary the temperature above T_g, and upon illumination, a more complete report on the subject will be published elsewhere [12].
For the deposition of macroscopically and microscopically homogeneous multilayers it is necessary to find optimal conditions for both Langmuir monolayer formation and its transfer on the substrate. We recorded the compression isotherms (Figure 1) both in dark and under UV illumination (provided with a filtered high pressure Hg lamp, λ=352nm), and deposited the films using a KSV5000 Langmuir trough of 10cm width. In particular we prepared the

sample as follows: 50μl of chloroform solution 1mg/ml of PA4 was spread on high purity water (MilliQ, ρ>18MΩcm), the Langmuir layer was then slowly compressed in dark at a rate of 10mm/min up to a typical deposition pressure Π=15mN/m. The multilayers were deposited either on clean Si (100) surfaces, covered by natural oxide (typical thickness 20-25Å, as determined by null-ellipsometry), or on silanized hydrophobic silicon. The wafers were first washed with soap and then cleaned in hot H_2SO_4. Silanization was performed by immersion of substrates in dimethyl-dichlorosilane/hexane and subsequent rinsing in hexane/acetone/hexane and final careful washing with soap and pure water. The hydrophobized substrates had a somewhat thicker oxide layer (25-30 Å by null-ellipsometry) coated by the non-polar $-CH_3$ group. Here we note that deposited films of

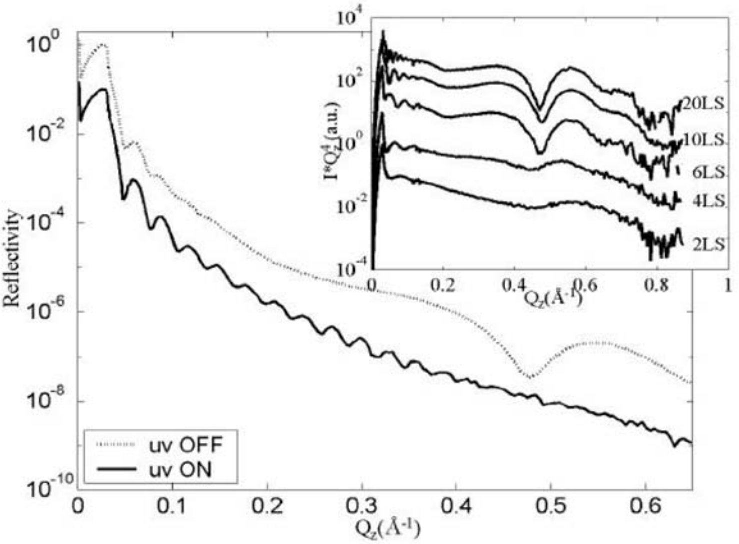

Figure 2: Photoinduced changes in the X-ray reflected intensity of a multilayer made of 10 layers of PA4 measured at T=RT . Dotted line: film before UV irradiation. Continuous line: film during UV irradiation. Note upon UV illumination the reduction of roughness, indicated by the extension of the Kiessig fringes, and the disappearence of the feature around Q_z=0.45$Å^{-1}$. **Inset:** X-ray reflectivity scaled by Q_z^4- for multilayers of different thickness (2, 4, 6, 10 and 20 layers) of PA4 deposited on natural silicon, measured at T=RT.

The Langmuir monolayers under compression were studied by following in real time the behavior of the ellipsometric parameters (at an angle of incidence Φ=40°, wavelength λ=632.8nm). For this we used a specially adapted small R&K trough, which was fit directly onto the light path of the ellipsometer. Here too the temperature could be controlled, and the effect of the azobenzene isomerization on the isotherms was studied by illuminating the Langmuir monolayer by a mercury lamp placed about 10 cm above the surface (see Fig. 1). As stated, we deposited several types of molecular architectures. The ones we have used for this study are:

- molecular multilayers of polymer deposited by the Langmuir-Schaefer technique on silicon substrate covered by its native oxide layer (typically 20-25 Å thick, roughness σ~3-4Å), giving rise to a weakly hydrophilic surface;
- molecular multilayers as above deposited onto silanized (hydrophobic) silicon substrate;
- superlattices obtained by the alternate deposition of fatty acid salts bilayers (e.g. barium behenate, BaBeh) by the Langmuir-Blodgett deposition technique and polymeric multilayers by the Langmuir-Schaefer technique. The substrate was previously hydrophobized by silanization. The structures thus obtained where $[2\text{BaBeh: nPA4}]_k$ with n=1,2,4 and k=12

X-ray reflectivity experiments were performed on the beamline ID10b (Troika-2) at the ESRF synchrotron facility operating at the wavelength λ=1.385Å. We constantly recorded rocking curves to test the level of diffuse background and discriminate the true specular reflectivity. In the following, data are truncated in Q_z in order to show the true specular reflectivity only.

The sample was placed in an helium-flushed chamber with the temperature controlled by means of a Peltier cell (temperature stability within ±0.1K). For the *cis-trans* isomerisation we used a filtered high pressure Hg lamp placed on top of the sample, at a distance of 10cm. Grazing incidence diffraction (GID) patterns were collected with incident beam impinging at an angle χ=0.18° on the sample surface, i.e. below the critical angle for total reflection of the substrate, which warrants that the observed GID signal originates from polymeric layer only. We integrated the signal in the vertical direction by means of a position sensitive detector (PSD) over the range Q_z from 0 to about 0.3 $Å^{-1}$.

3. RESULTS AND DISCUSSION

In the inset of Figure 2 we show the reflectivity curves measured on a set of multilayers composed of 2, 4, 6, 8, 10 and 20 layers of PA4 deposited on Si covered by its natural oxide. The total film thickness can be easily evaluated from the Kiessig fringes, which appear above the critical angle, and are due to the interference between the waves reflected at the air/film and the film/substrate interfaces. The distance between adjacent minima is $\Delta Q_Z=2\pi/D$ where D is the film thickness. The values of D that we obtain (D=21-22Å per

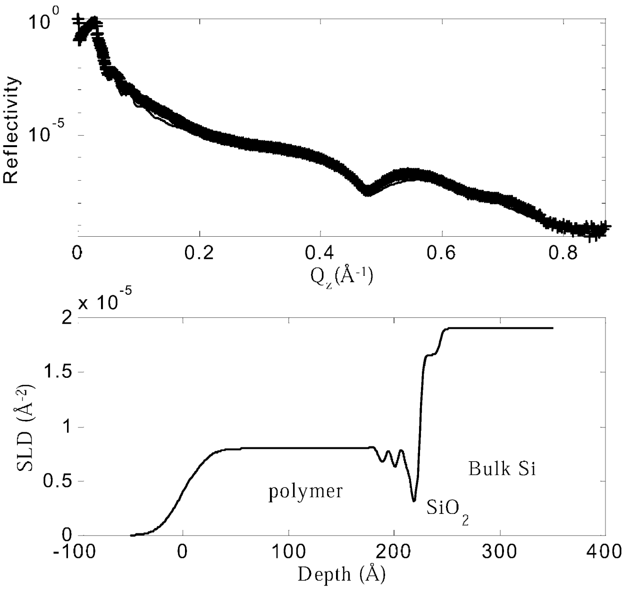

Figure 3: **Top panel:** Fit (continuous line) of the reflectivity curve (crosses) of a multiplayer (10 layers) of PA4 at T=RT. **Bottom panel:** The model of Scattering Length Density (SLD=$r_0\rho_e$, Å^{-2}, see text for details) employed to fit the experimental data.

layer) are in agreement with our ellipsometric measurements [8] while the observed roughness (σ=15-20 Å) corresponds to an incomplete coverage of the topmost monolayer. The latter finding is in agreement with the results of recent non-contact AFM measurements performed on the same multilayers [12].

It is interesting to note the presence of a feature peaked at $Q_Z \sim 0.48$Å^{-1}, in the reflected intensity which develops in the curves from multilayers with n>4 layers. This value of Q_z would correspond in the direct space to a periodic feature of about 13-14Å. The exposure of the sample to UV radiation, which is known to induce *trans* to *cis* isomerization of the azobenzene side-group, causes the disappearance of the feature in the reflectivity pattern, as shown in figure 2.

The other remarkable effect shown in the same figure is the extension of the Kiessig fringes to much higher Q_z values than in pristine LS multilayers. This implies smoothing of the polymer-air interface: the value for the surface roughness reduces to $\sigma \approx 10$Å, as obtained by the fit of the Kiessig fringes region. The present 'smoothing' effect is again confirmed by our non-contact AFM measurements.

Coming now to the 'dip' in the reflected intensity observed at $Q_z \sim 0.48$Å^{-1}, which is related to the internal structure of the film, we must note that in general the interpretation of a reflectivity pattern from a structured film is not unique, due both to the lack of information on the phases of the various contributions to the reflected intensity, and to the necessarily limited accessible Q-range, which in turn is limited by the signal-to-noise ratio, and by the given instrumental background contribution.

From the point of view of monochromatic incident X-rays of wavelength λ, ignoring absorption, each layer of the film is represented by its index of refraction $n=1-(\lambda^2/2\pi\, r_0\rho_e)$ where $r_0=2.81*10^{-5}$Å is the classical electron radius and ρ_e is the electron density in Å^{-3}; typically n differs from unity by a quantity of the order of magnitude of 10^{-5}-10^{-6} [13]. The

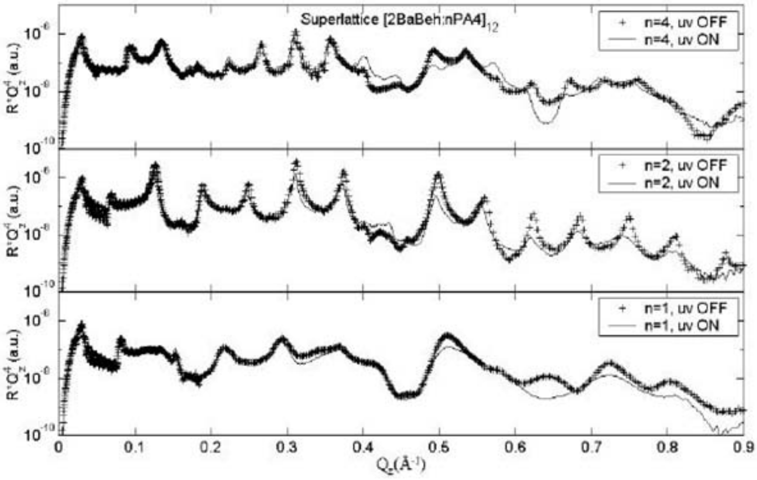

Figure 4: reflectivity curves scaled by the fourth power of the exchanged momentum Q_z, as measured on ID10b, before and during UV irradiation at room temperature of the superstructures $[2\text{BaBeh: nPA4}]_{12}$, with n=4,2, and 1 (top, middle and bottom panels respectively).

intensity R of radiation reflected by a single interface between media 0 and 1 is given by the usual Fresnel expression [14]:

$$R = |\,(n_0\sin\theta_0 - n_1\sin\theta_1) / (n_0\sin\theta_0 + n_1\sin\theta_1)\,|^2$$

where n_0 and n_1 indicate the refractive indexes of media 0 and 1 respectively, θ_0 is the incidence angle and θ_1 the diffraction angle, determined by Snell's law. Below the critical angle $\theta c = acos(n_1/n_0)$ the incoming radiation is totally reflected (R=1), whereas at large incidence angle the asymptotic law $R \sim Q_z^{-4}$ is observed.

We calculate the intensity reflected by a complex layered structure by applying either the matrix approach or the recursive Parrat algorithm [15]. Layer roughness is accounted for by the Nevot-Croce approximation [16], appropriate for roughness with small (< 1μm) lateral coherence. Such approach requires a preliminary guess about the elements of the model. This can be done by inverse Fourier Transformation (FT) of the reflected intensity R(Q), which is, in the kinematic (Born) approximation, simply related to the modulus of the FT of the gradient of the refractive index:

$$R(Q)=R_F \left| \int (\partial n/\partial z\} \exp(iQ_z)\, \partial z \right|^2$$

Therefore- after careful normalization- one can hope to be able to extract, in a model-free fashion, the distances between the various interfaces.

For the interpretation of the internal structure of the polymeric film we first obtained an ansatz model by applying inverse FT to the measured reflectivity. After normalization to the reflectivity of bare substrate, we obtained a structured (layered) variation in the refractive index, which is associated with the 'typical' distances of 23, 37 and 50Å. We then refined this model either by using the Parrat32 software [17] or double checking our results with software developed by one of us [18]. The resulting theoretical intensity and structural model are shown in Figure 3, top and bottom panels respectively. The substrate is modeled as bulk Si covered by 19Å thick native oxide, whose scattering length density ($SLD=r_0\rho_e$) values are known from the literature. The polymeric film is made up of a first series of pseudo-periodic, layered units of thickness 13.5Å, with zones of alternating high and low SLD. In particular the interface between the silicon oxide and the polymer shows a minimum SLD density, followed by a region of higher density. This structure is repeated 3 or 4 times with decreasing contrast between high SLD and low SLD regions. At large distance from the substrate the polymeric film is unstructured and has an average SLD $\sim 0.9*10^{-5}$Å^{-2}, a reasonable value if compared to that of pure PMMA (SLD = $1.08*10^{-5}$Å^{-2}, [19]). The film-air interface has roughness $\sigma \sim 20$Å.

Similar results were also found for films deposited onto silanized hydrophobic substrates. We note in passing that other possible models, such as crystalline regions embedded in an amorphous matrix, have been discarded on the basis of all the other knowledge that we have on this polymeric system.

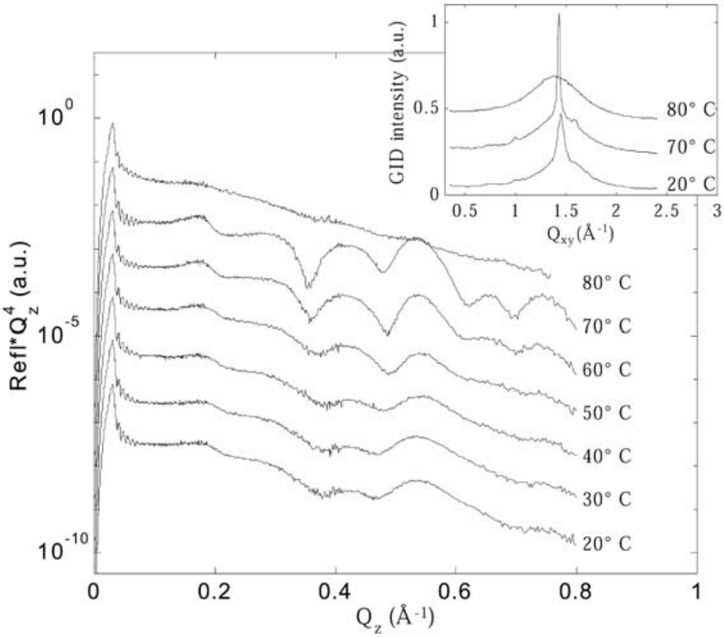

Figure 5: reflectivity curves of 40 monolayers of PA4 as a function of the temperature. The onset of the nematic phase and its melting are responsible for the appearance of the features at Q_z>0.3Å^{-1} and their evolution. **INSET:** GID pattern from a similar sample at selected temperatures. It is evident from the data that the nearest neighbor correlation peak sharpens upon heating until the final melting of the multilayer is reached at about 80°C.

Coming now to the superlattice structures, in Figure 4 we report the reflectivity curves scaled by the fourth power of the exchanged momentum Q_z^4, as measured before (crosses) and during (line) uv irradiation at room temperature from the superstructures [2BaBeh: nPA4]$_{12}$, with n=1,2, and 4 (bottom, middle and top panels respectively).

In general we note that the effect of UV-illumination is that of reducing the contrast smearing out and reducing the intensity of the higher order Bragg peaks observed above Q_z ~ 0.4 Å^{-1}. Moreover, the photo-expansion effect we observe is markedly reduced with respect to the same effect observed in pure PA4 azopolymer molecular multilayers, although it is not completely disappearing. The first effect is easily understandable considering that the photoinduced isomerization of the azo-moieties induces overall dynamics and disorder in the molecular superlattice sandwich, therefore reducing the contrast responsible for the observation of the Bragg peaks. On the contrary, the second observed effect, i.e. the reduced photo-expansivity, can be connected with the ordering effect induced by the fatty acid molecular sandwiches, and to the reduced role of free surface in inducing molecular motion in such superlattices. Investigation is currently in progress on the same superstructures by null-ellipsometry in order to understand the role of free surface and extra induced molecular order in determining both the amplitude of the photo-expansion and the back-to-equilibrium relaxation kinetics.

In Figure 5 we show the reflectivity scaled by the 4th power of the exchanged momentum Q_z^4, for a multiplayer (40 layers) of PA4 as a function of temperature, data are taken upon heating. The development of the structures at $Q_z > 0.3Å^{-1}$ in the reflectivity curves measured above 40-50°C is related to the onset of the glass to nematic phase transition, occurring at 78° C. The melting of the glassy phase results in the flat, featureless reflectivity curves measured at T=80° C, which implies a disruption of the periodicity along the *z* direction, typical of the nematic phase. We note in passing that the roughness of the top and bottom interfaces is the same for all the temperatures, as can be evaluated by the damping cutoff of the Kiessig fringes. In the inset of the same Figure 5 we also report the GID signal obtained from a multiplayer (6 layers) film of PA4 deposited onto hydrophobic Si, at different temperatures. While at T=20°C the GID signal consists mainly of one broad peak of almost Lorentzian shape centered at $Q_{xy}=1.44$ $Å^{-1}$, as the temperature is increased the GID peaks become narrower and better defined, and two much weaker shoulders appear around $Q_{xy}=1.0Å^{-1}$, and $1.65Å^{-1}$. The change of the GID signal is consistent with that of the reflectivity curve: the sample becomes better structured as the temperature is increased, before melting, both in the normal to surface and in the in plane direction. Moreover we can infer that a minority part of our sample undergoes crystallization upon heating, as we observe a transition from hexagonal packing to a generic monoclinic cell, while all the rest remains in a liquid like state –giving rise to the broad background observed under the sharp peak in the GID pattern. This latter point is under current investigation. Finally at T=80° C the sample becomes nematic, with no long-range positional order, and a broad unstructured peak appears, characteristic of this phase.

4. CONCLUSIONS.

We have investigated, by X-ray reflectivity and GID, the morphological and structural changes induced by photo excitation of homo- and heterostructures of an azobenzene side chain liquid crystalline polymer. We observed extensive photoinduced effects on the nanoscale: expansion of the multilayers independently of number of layers, reduction of surface roughness, and destruction of order to yield a glass-like phase. We have also found that molecular aggregation (as it is the case for the first layers closer to the substrate) is connected with large modifications of the dynamical properties, eg. back-to-equilibrium relaxation time. In superlattices composed of alternate layers of barium behenate and photosensitive polymer we found a general reduction of photoinduced structural effects.

References

[1] C. B. Mc Ardle ed., Side Chain Liquid Crystal Polymers, Blackie and Sons, Glasgow,(1989);
A.Blumstein ed., Polymeric Liquid Crystals, Plenum Press, NewYork, 1985;
N.A. Plate' ed., Liquid-Crystal Polymers, Plenum Press, NewYork, 1993.
[2] S. Kumar Chem.Rev. **89**, 1915 (1989)
K. Anderle , R. Birenheide , M. J. A. Werner , J. H. Wendorff Liquid Crystals **9**, 691 (1991)
[3] J. P. Hansen , D. Levesque , J. Zinn-Justin eds., Liquids, Freezing and Glass Transition, North Holland, Amsterdam (1991);
W. Gotze, J. Phys.: Cond. Mat., **11**, A1 (1999).
L. Cristofolini, P. Facci, P. Camorani, M. P. Fontana. J. Phys.: Cond. Mat., **11** A359 (1999)
[4] L. Cristofolini, M.P. Fontana, O. Konovalov - Philosophical Magazine B **82**, xxx (2002).
[5] S. Arisi,P. Camorani, L. Cristofolini, M.P. Fontana, M. Laus, Mol. Cryst. Liq. Crystal., in press (2001)
[6] L. Cristofolini, M.P. Fontana, M. Laus B. Frick - Phys. Rev. E, **64,** 080112 (2001)
[7] G. Roberts ed. Langmuir-Blodgett Films, Plenum Press, New York, (1990)
A.Ulman ed. Ultrathin Organic Films, Academic Press, Boston (1991)
[8] L. Cristofolini, S. Arisi, M. P. Fontana - Phys. Rev. Letter **85**, 4912 (2000)
L. Cristofolini, S. Arisi, M. P. Fontana - Synth. Metals **124**, 151 (2002).
[9] A. S. Angeloni, D. Caretti, C. Carlini, E. Chiellini, G. Galli, A. Altomare, A. Solaro, M. Laus, Liquid Crystals, **4**, 513 (1989)
[10] L. Andreozzi, M. P. Fontana, F. Francia, M. Giordano, D. Leporini, M. Rateo, J. Non-Cryst. Solids, **172**, 943 (1994)
[11] R.A.L. Jones, R.W. Richards, Polymers at surfaces and Interfaces.Cambridge University Press, Cambridge (1999)
[12] L. Cristofolini et al., in preparation.
[13] J. Daillant, A. Gibaud eds, X-ray and neutron Reflectivity: principles and applications, Springer, Berlin (1998)
[14] M. Born, E. Wolf Principles of Optics, 7th edition Cambridge University Press, Cambridge (1999)
[15] L. G. Parrat Phys. Rev. B **95**,359 (1954)
[16] L. Nevot , P. Croce Revue de physique appliquee, **15**, 761 (1980)
[17] C. Braun, Parrat32 Software for reflectivity, HMI Berlin (1999)
[18] O.V. Konovalov, L.A. Feigin, B.M. Shchedrin. Kristallografiya, **41**, 640 (1996); O.V. Konovalov, I.I. Samoilenko, L.A. Feigin, B.M. Shchedrin Kristallografiya, **41**, 635 (1996)
[19] M. Stamm, G. Reiter, K. Kunz, Physica B **173**, 35 (1991)